Hidden Charge Orders in Low-Dimensional Mott Insulators

applied sciences

MDPI

Review

Hidden Charge Orders in Low-Dimensional Mott Insulators

Serena Fazzini † **and Arianna Montorsi** *

Institute for Condensed Matter Physics and Complex Systems, DISAT, Politecnico di Torino, I-10129 Torino, Italy; serena.fazzini@polito.it

* Correspondence: arianna.montorsi@polito.it

† Current address: Department of Physics and Research Center OPTIMAS, University of Kaiserslautern, D-67663 Kaiserslautern, Germany.

Received: 7 December 2018; Accepted: 13 February 2019; Published: 22 February 2019

Abstract: The opening of a charge gap driven by interaction is a fingerprint of the transition to a Mott insulating phase. In strongly correlated low-dimensional quantum systems, it can be associated to the ordering of hidden non-local operators. For Fermionic 1D models, in the presence of spin–charge separation and short-ranged interaction, a bosonization analysis proves that such operators are the parity and/or string charge operators. In fact, a finite fractional non-local parity charge order is also capable of characterizing some two-dimensional Mott insulators, in both the Fermionic and the bosonic cases. When string charge order takes place in 1D, degenerate edge modes with fractional charge appear, peculiar of a topological insulator. In this article, we review the above framework, and we test it to investigate through density-matrix-renormalization-group (DMRG) numerical analysis the robustness of both hidden orders at half-filling in the 1D Fermionic Hubbard model extended with long range density-density interaction. The preliminary results obtained at finite size including several neighbors in the case of dipolar, screened and unscreened repulsive Coulomb interactions, confirm the phase diagram of the standard extended Hubbard model. Besides the trivial Mott phase, the bond ordered and charge density wave insulating phases are also not destroyed by longer ranged interaction, and still manifest hidden non-local orders.

Keywords: hidden orders; Mott insulators; Hubbard model

1. Introduction

As predicted by sir Neville Mott almost seventy years ago [1], interaction is capable of opening energy gaps in bands of otherwise conducting materials, so that at sufficiently low temperature they become insulating. The microscopic arrangement of the electronic degrees of freedom consistent with such insulating phase, as well as the corresponding macroscopic orders, have been more elusive. In fact, classical local order parameters, such as magnetic or charge order, are often vanishing both in the metallic and in the insulating state of low-dimensional insulators. This is the case for instance for the Mott phase of the paradigmatic Hubbard model. In one dimension, and at zero temperature, it takes place for any non-zero value of the on-site Coulomb repulsion. Only recently [2] it was proved that, despite the absence of a local order parameter, the insulating phase is characterized by the ordering of a non-local (NL) parity operator. The result has been successively extended also to ladders [3], and to the two-dimensional bosonic case [4]. For Fermions in 1D, it was also proved on more general grounds by means of a bosonization analysis and a renormalization-group (RG) study of the continuum limit that, in the case of spin–charge separation and local interaction, in each (spin or charge) channel, the two possible gapped phases are univocally associated to the non-vanishing of the expectation value of one of two hidden NL operators: string or parity [2,5,6]. The result provides a clear insight into the basic

microscopic structure of the possible insulating phases induced by interaction through the opening of a gap in the charge channel. For instance, the non-zero expectation value of the NL parity tells us that the Mott insulating phase of the Hubbard model amounts to a uniform background of singly occupied sites in which empty (holons) and doubly occupied (doublons) sites are charge fluctuation appearing only in correlated pairs of finite coherence length. In addition, a more peculiar "topological" Haldane-like ordering of holons and doublons can occur in the insulating phase of other lattice models, and is characterized by the non-vanishing of the NL string order.

The above bosonization predictions apply to short-ranged (on-site or local) interactions, and can be verified in ultracold systems of Fermionic atoms trapped onto optical lattices. In particular, NL order parameters can be measured by means of in-situ imaging techniques, as in [7,8]. For more general applications in both condensed matter and atomic physics, it would be interesting to understand how such orders and phases are modified by the presence of a long-ranged interaction, i.e., an interaction decaying with distance r as $r^{-\alpha}$, with $\alpha > 0$. This is the case for instance for both dipolar interaction ($\alpha = 3$), and unscreened Coulomb repulsion ($\alpha = 1$). In fact, when the decay is sufficiently fast ($\alpha > 1$), it is expected that the phase diagram remains qualitatively the same [9], and a similar behavior is derived also for the non-local parameters [10]. However, it is not possible to obtain analogous analytic predictions for lower α's values.

In this article, we first review the general classification of the possible one-dimensional insulating phases for Fermionic systems described by a double sine Gordon Hamiltonian in terms of hidden orders. We then summarize how insulating phases characterized by a parity order can also be found in two-dimensional systems, upon appropriate generalization to branes of fractional parity. We discuss how instead a finite value of solely the string charge operator is peculiar of the Haldane insulating phase and is accompanied by fractionalized edge modes in the charge channel. Finally, we specialize our discussion to the repulsive extended Hubbard model at half-filling. We add to the model diverse long-ranged interaction (dipolar, screened and unscreened Coulomb) and compare the preliminary results obtained by means of density-matrix-renormalization-group (DMRG) numerical analysis. In particular, we explore at fixed large L the changes at the phase transitions among Mott, bond-ordered-wave (BOW), and charge density wave (CDW) phases, as well as the capability of NL order parameters to capture all of them.

2. Non-Local Orders in Interacting Low Dimensional Insulators

2.1. Sine Gordon Hamiltonian in One Dimension

The low-energy physics of a wide class of 1D interacting Fermionic systems at half band filling is characterized by spin–charge separation. This is well captured by an effective Hamiltonian consisting of two decoupled sine-Gordon models describing the charge and spin channels, respectively:

$$\mathcal{H}_{SG} = \sum_{\nu=c,s} \int dx H_\nu(x) \tag{1}$$

with

$$H_\nu = H_{0\nu} + \frac{m_\nu v_\nu}{2\pi a^2} \cos(\sqrt{8\pi}\phi_\nu) \tag{2}$$

and

$$H_{0\nu} = \frac{v_\nu}{2}\left[K_\nu(\partial_x\theta_\nu)^2 + \frac{1}{K_\nu}(\partial_x\phi_\nu)^2\right] \tag{3}$$

Here, $\Pi_\nu = -\partial_x\theta_\nu$ is the conjugate momentum of the field ϕ_ν. The mass coefficients m_ν, the Luttinger parameters K_ν and the velocities v_ν depend on the coupling constants and the filling of the corresponding microscopic lattice Hamiltonian [9,11]. Each channel $\nu = c, s$ of the model in Equation (2) is characterized by a competition between the $H_{0\nu}$ term in Equation (3), which describes an harmonic oscillator with fluctuating field ϕ_ν, and the cosine term, which would favor the pinning of

the field around a locked value. Such competition leads to the appearance of different physical phases, as described below.

The microscopic lattice Hamiltonian corresponding to Equation (1) is formulated instead in terms of Fermionic operators $c_{j\sigma}$, with j denoting the lattice site and $\sigma = \uparrow, \downarrow$ the spin. The connection between the continuum model in Equations (1) and (2) and the underlying lattice models relies on the idea that in most relevant situations the physically interesting energy range of a lattice model is small as compared to the whole bandwidth. It is then customary to introduce an effective model that is equivalent to the lattice model in the low-energy sector. To this purpose, one first rewrites the starting lattice Hamiltonian in terms of four Fermionic fields $\psi_{\alpha\sigma}(x)$ on the continuum, with $\alpha = \pm 1$ referring to the two Fermi points $\pm k_F$, related to the lattice operators via $\psi_{\alpha\sigma}(x) = \sum_{k \simeq \alpha k_F} e^{ikx} c_{k\sigma}$, where $c_{k\sigma}$ are the Fourier components of the original lattice operators $c_{j\sigma}$. Then, by adopting the bosonization formalism [9,11], one re-expresses the four Fermionic fields as vertex operators $\psi_{\alpha\sigma} = \eta_{\alpha\sigma} \exp\left[i\sqrt{\frac{\pi}{2}}(\alpha\phi_c + \alpha\sigma\phi_s + \theta_c + \sigma\theta_s)\right] / \sqrt{2\pi a}$, where ϕ_ν, θ_ν (with $\nu = c, s$) is a pair of bosonic fields related to charge (c) or spin (s) degrees of freedom, a is a short-distance cut-off, and $\eta_{\alpha\sigma}$ are anti-commuting Klein factors. By applying this method, e.g. to the Hubbard model, which describes the competition of a band "hopping" term and an "on-site" two-body Coulomb repulsion with coefficient U, the model in Equations (1) and (2) is obtained, with $m_\nu \propto U$. The same model is found for a wide class of extended Hubbard-like models that include further interaction beyond the on-site approximation, such as nearest neighbor diagonal interaction, correlated hopping, pair hopping and so on [12–15] , as well as three- and four-body interactions [6] that may be relevant in ultracold atoms or molecules trapped in optical lattices.

2.2. Classification of Insulating Phases

For the above reasons, the sine-Gordon model in Equations (1)–(2) plays a crucial role in the characterization of 1D Fermion lattice models. The result of the competition of the two terms appearing in Equation (2) depends on the sign and the magnitude of the mass term m_ν in each channel ν, and can be established by a well known RG analysis of the sine-Gordon model [11]. In brief, for $4(\sqrt{K_\nu} - 1) < |m_\nu|$, the cosine term becomes relevant, and a gap opens in the related channel $\nu = c, s$, with the field ϕ_ν pinned at either 0 (for $m_\nu < 0$) or $\pm\sqrt{\pi/8}$ (for $m_\nu > 0$). The case where no gap opens in both channels corresponds to the Luttinger liquid (LL) phase, where ϕ_c and ϕ_s are both unpinned and the effective Hamiltonian is $H_{LL} = \sum_\nu \int H_{0\nu}$. The remaining eight phases, are characterized by a gap in at least one channel. To classify all possible insulating phases, one should focus on the cases in which the charge gap is open, i.e., the charge field is pinned. These are summarized in Table 1, with the pinning value of the fields provided in the first and second columns.

Table 1. Left-hand side: Classification of the insulating phases for $\mathcal{H}_{SG}$ at half-filling. The first column denotes the two possible pinning values for the charge ($\phi_c(x)$) field. The second gives the value of the spin field, with u standing for "unpinned". The third column denotes the non-vanishing NL order parameters $\mathcal{O}^\nu_{\mathcal{A}}$, $\nu = c, s$. Right-hand side: The phase without topological features are denoted by "triv", whereas we report the type of symmetry (T and or P) protecting the phases with degenerate edge modes.

	$\sqrt{8\pi}\phi_c$	$\sqrt{8\pi}\phi_s$	NLO	SP
Mott	0	u	$\mathcal{O}^c_{\mathcal{P}}$	triv
HI	$\pm\pi$	u	$\mathcal{O}^c_{\mathcal{S}}$	P, T
BOW	0	0	$\mathcal{O}^c_{\mathcal{P}}$, $\mathcal{O}^s_{\mathcal{P}}$	triv
CDW	$\pm\pi$	0	$\mathcal{O}^c_{\mathcal{S}}$, $\mathcal{O}^s_{\mathcal{P}}$	P
SDW	0	$\pm\pi$	$\mathcal{O}^c_{\mathcal{P}}$, $\mathcal{O}^s_{\mathcal{S}}$	P, T
BSDW	$\pm\pi$	$\pm\pi$	$\mathcal{O}^c_{\mathcal{S}}$, $\mathcal{O}^s_{\mathcal{S}}$	P

In the table, the denomination of the different insulating phases is borrowed form the one adopted in the case of some correspondent lattice model. Indeed, it is possible to see [9] that the phase denoted here as Mott is the one characteristic of the repulsive Hubbard model at half-filling, with no local order and dominant spin density wave (SDW) correlations. Similarly, the other partly gapped insulating phase, which we denote as Haldane insulator (HI) for reasons clarified below, corresponds to no local order and dominant CDW correlations. Both are characterized by the presence of a gap in only the charge channel. In contrast, BOW, CDW, spin density wave (SDW), and bond spin density wave (BSDW) are fully gapped phases, also characterized by a gap in the spin channel and by a finite local order parameter. In these latter cases, in the ground state, a spontaneous symmetry breaking can be observed. The explicit expression of the parameters in $\mathcal{H}_{SG}$ in terms of the coupling constants of the microscopic Hubbard-like models are given in previous works [6,12,13,16] and are not reported here. As an example, in the next section, we discuss in more details the lattice model with diagonal density–density interaction, also known as extended Hubbard model.

2.3. Non-Local Orders

The standard way of characterizing the physical features of different ordered phases is to analyze the asymptotic behavior of correlation functions of appropriate local operators. In 1D, they asymptotically decay to zero with a power or exponential law: the "order" of the phase is described by the correlation function which decays slower, except when the ground state spontaneously breaks some discrete symmetry of the Hamiltonian. Only in the latter case, one of the correlation functions remains finite, thus capturing the long range order of the phase through a local operator, whose expectation value can be regarded to as an order parameter.

Recently it has been realized [2,5,17] that, even when the Hamiltonian has only continuous internal symmetries, non-local operators may order in some phases, meaning that their average value is non-zero in these phases and vanishes at the phase transition. Importantly, such operators turn out to be non-local in the lattice representation, which is consistent with the absence of spontaneous symmetry breaking. They can be built by means of the on site charge and spin density operators $s_{\nu j}$, here defined as $s_{cj} = (n_{j\uparrow} + n_{j\downarrow} - 1)/2$, and $s_{sj} = (n_{j\uparrow} - n_{j\downarrow})/2$, $n_{j\sigma} \doteq c^\dagger_{j\sigma} c_{j\sigma}$ being the Fermion number operator at site j with spin σ. Upon introducing the on-site parity $P^\nu_j \doteq \mathrm{e}^{2\pi i s_{\nu j}}$ ($P_\nu = \pm 1$), one can finally define two NL operators as

$$\mathcal{O}^\nu_{\mathcal{P}}(r) = \prod_{j=1}^{r} P^\nu_j \quad , \quad \mathcal{O}^\nu_{\mathcal{S}}(r) = 2 s_{\nu r} \prod_{j=1}^{r-1} P^\nu_j \tag{4}$$

with asymptotic correlation functions

$$\mathcal{C}^\nu_{\mathcal{A}} = \lim_{r\to\infty} \underbrace{\langle \mathcal{O}^{\nu\dagger}_{\mathcal{A}}(0)\, \mathcal{O}^\nu_{\mathcal{A}}(r) \rangle}_{\mathcal{C}^\nu_{\mathcal{A}}(r)} \tag{5}$$

with $\mathcal{A} = \mathcal{P}, \mathcal{S}$. In each channel, the operators $\mathcal{O}^\nu_{\mathcal{A}}(r)$ are better known as parity ($\mathcal{A} = \mathcal{P}$) and string ($\mathcal{A} = \mathcal{S}$) operators, respectively. It turns out that the non-vanishing of the average of one of the two operators in the charge channel, together with the behavior of their companions in the spin channel are able to capture all the possible insulating phases that may be induced by interaction in these systems. This is shown in column NLO of Table 1, where for each phase it is reported which NL operators are non-vanishing.

The above results may be understood in the continuum limit by evaluating the NL operators in Equation (4) in terms of the bosonic fields. They read [2,17]:

$$\mathcal{O}^\nu_{\mathcal{P}} \sim \cos(\sqrt{2\pi}\phi_\nu) \quad , \quad \mathcal{O}^\nu_{\mathcal{S}} \sim \sin(\sqrt{2\pi}\phi_\nu) \quad . \tag{6}$$

Unlike the case of local operators, each of the above NL operators is associated to a single bosonic field. Thus, while their averages, as well as the correlation functions in Equation (5), are all vanishing when both fields are unpinned (LL phase), if some field is locked to a fixed value, at least one NL operator has non-zero average. More precisely, in each channel, when the field ϕ_ν is pinned to one of the two possible values in Table 1, the average of one of the two corresponding NL operators becomes finite, whereas the other remains identically zero. It is straightforward to verify that in both cases just one of the correlation functions $\mathcal{C}^\nu_\mathcal{P} \propto \langle \cos\sqrt{2\pi}\phi_\nu\rangle^2$, $\mathcal{C}^\nu_\mathcal{S} \propto \langle \sin\sqrt{2\pi}\phi_\nu\rangle^2$ remains finite [2], whereas the other one still vanishes. The average values of $\mathcal{O}^\nu_\mathcal{A}$ ($\mathcal{A} = \mathcal{P}, \mathcal{S}$) are thus identified as order parameters in the ν channel for the two possible gapped phases. In this way, the bosonization description is able to associate appropriate NL orders to each partly or fully gapped phase, as summarized in particular for the insulating phases in the third column of Table 1.

The discrete lattice expressions in Equation (4) of $\mathcal{O}^\nu_\mathcal{A}$ clarify the different microscopic arrangements of the related degrees of freedom in the two gapped phases in each channel. To understand the issue, we stress that the charge fluctuations are described by the local configurations with $2s_{cj} = \pm 1$, i.e., empty sites (holons) and doubly occupied sites (doublons), respectively. The spin fluctuations are characterized by $2s_{sj} = \pm 1$, i.e., sites occupied by a single electron with either up or down spin. Thus, the finiteness of the Haldane string correlator $\mathcal{C}^\nu_\mathcal{S}$ implies that for $\nu = c$ in the HI phase holons and doublons are alternated (i.e., between two successive doublons there is always a holon) and intercalated by an arbitrary number of single Fermions. Since this is the very same behavior of spins ± 1 in the Haldane phase of spin 1 models, the phase is usually denoted as Haldane insulator. A non-vanishing value of the parity operators in the charge channel denotes instead a state in which all the sites are singly occupied, as in the case of the infinite-U repulsive Hubbard model, or when they are not the parity breaking sites occur in entangled pairs of holons and doublons with finite coherence length.

2.4. One Dimensional Topological Mott Insulators

In particular, in the case of the HI phase , one can prove that at the edge sites a fractional charge always accumulates [18], differing from the bulk one. In fact, while the average on-site charge is one, two degenerate states with non-integer charges $e^{(\pm)}(x_\chi)$ occur at the left ($\chi = -$) and right ($\chi = +$) edges. At half-filling, within the bosonization approach, such charges can be evaluated as the average charge plus the charge kink at the edge. Explicitly,

$$e^{(\pm)}(x_\chi) = 1 + 2 \lim_{a\to 0^+} \frac{1}{\sqrt{2\pi}} [\phi_c(x_\chi) - \phi_c(x_\chi - a)] = 1 \pm \frac{\chi}{2} \quad , \tag{7}$$

where the sign $\pm$ descends from the pinning value of the charge field, also reported in first column of Table 1. More precisely, one of the two degenerate states has a left-edge charge equal to $3/2$ and a right-edge charge equal to $1/2$, whereas the other has the opposite arrangement. This is qualitatively reproduced in the cartoon shown in Figure 1.

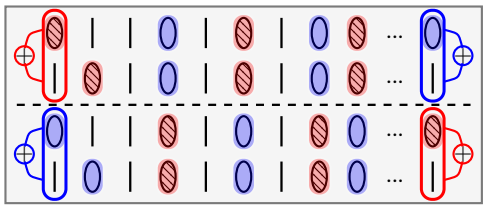

Figure 1. Cartoon of the Haldane phase, showing the presence of two degenerate states with fractional edge modes. The Haldane order consists of the superposition of all possible configurations with a string of alternated holons (empty blue circles) and doublons (patterned red circles) diluted in a background of single electrons with arbitrary spin orientation (black lines). For an open chain, the string starting with the doublon (**top**) and that starting with the holon (**bottom**) are distinct states. Therefore, each edge acquires a fractional charge given by the superposition of either doublons and single occupations or holons and single occupations.

The two states with non-trivial topology cannot be deformed adiabatically one into the other without closing the gap, nor into the trivial Mott insulator state, characterized by the non-vanishing of the charge parity. Thus, the phases are distinct. This is true at least in the presence of particle–hole (P) symmetry, which action on the bosonic fields $\phi_\nu(x)$, $\theta_\nu(x)$ can be expressed as

$$P\phi_\nu P^{-1} = -\phi_\nu \ , \ P\theta_\nu P^{-1} = -\theta_\nu \quad . \tag{8}$$

From the above relations, one verifies that P is a symmetry of both H_νs. Moreover, to change adiabatically the pinning values of the field ϕ_ν one into the other, one must break such symmetry. Hence, P configures as the symmetry protecting the topological nature of the phase.

We emphasize that both the phases classification reported in Table 1 and the above topological properties (7) of the ground state of the Hamiltonian are obtained from the RG analysis of its asymptotic behavior and its symmetries. However, the topological aspects can also be understood [18] within the more general framework of symmetry protected topological phases [19–22]. In the last column of Table 1, for each of the insulating phases, it is shown which are the internal symmetries protecting the non-trivial phases, whereas triv indicates the phases with trivial topological properties. Moreover, T denotes the time reversal symmetry, which action reads:

$$T\phi_\nu T^{-1} = \delta_\nu \phi_\nu \ , \ T\theta_\nu T^{-1} = -\delta_\nu \theta_\nu \tag{9}$$

with $\delta_c = 1$, $\delta_s = -1$.

2.5. Fractional Parity Orders in Trivial Low Dimensional Mott Insulators

The possibility to generalize to higher dimension the Haldane insulating phase, with its non-trivial topological nature, strongly relies on the lattice geometry. In particular, in the case of spinful electrons on a square lattice, it is not possible to obtain such topological phase.

It is much easier instead to generalize to higher dimension the trivial Mott insulating phase, characterized in the one dimensional case by a non-vanishing value of the charge parity operator. As already mentioned, its physics amounts to a background of singly occupied sites, in which holons and doublons occur in entangled pairs with a finite coherence length. These in principle can occur in arbitrary dimension. A two-dimensional example is depicted in the cartoon of Figure 2. In presence of such physics, the parity operator must be properly generalized in order to remain non-vanishing in the insulating phase, and zero elsewhere. Let us start with the case of a M legs ladder: rather than considering a string of site parities delimited by two boundary sites, as in the definition in Equations (4) and (5), one now takes *branes* of sites delimited by boundary strings, as proposed in [23]. Explicitly, we can introduce:

$$O_P(r, M) = \prod_{0 \le x < r} \prod_{0 \le y < M} \mathcal{P}^c_{x,y} \tag{10}$$

where x, y denote the coordinates of sites.

Even with the above generalization of the parity operator, an increase of the length of the boundary turns out to diminish its average value also in the insulating phase. In fact, the longer the boundary, the higher the number of holon–doublon pairs divided by it, which are responsible for the switch of the parity sign. Such effect has been quantified as a "perimeter law": the parity decreases to zero in the two-dimensional limit $M \to \infty$ with $e^{-\pi b M}$, where b is a positive constant and M is the length of the boundary. To overcome such difficulty, a fractional generalization of the brane parity was introduced [4], in which the site parities are multiplied by a fractional angle π/M^{α}, instead of π characteristic of the one-dimensional case. Explicitly, one defines a generalized brane parity operator as:

$$O_P^{(\alpha)}(r, M) \equiv [O_P(r, M)]^{(\frac{1}{M})^{\alpha}}, \tag{11}$$

where α possibly depends on the model Hamiltonian. It turns out that the insulating phase of the two-dimensional Hubbard model is characterized by a non-vanishing value of its expectation value. More precisely, by first taking $r = L/2$ and then the limit $L \to \infty$, one can prove that:

$$C_P^{(\alpha)} \doteq \lim_{M\to\infty} \lim_{L\to\infty} \langle O_P^{(\alpha)}(L/2, M)\rangle \tag{12}$$

is finite, solely in the MI phase, for $\alpha \geq \frac{1}{2}$, in the bosonic case. In fact, it is exactly equal to 1 in case the inequality is strict, whereas its finite value depends on the Coulomb repulsion U for $\alpha = 1/2$.

A similar result holds also for the Fermionic 2D Hubbard model at half filling [24]. Noticeably, in the latter case, it is found that also the fractional spin parity, defined in full analogy with Equation (10) upon replacing $\mathcal{P}^c \to \mathcal{P}^s$, remains finite. This fact turns out to be crucial to the onset of d-wave superconductivity away from half filling, where the fractional charge parity vanishes while the spin one remains finite in the same range of values in which superconductivity is present.

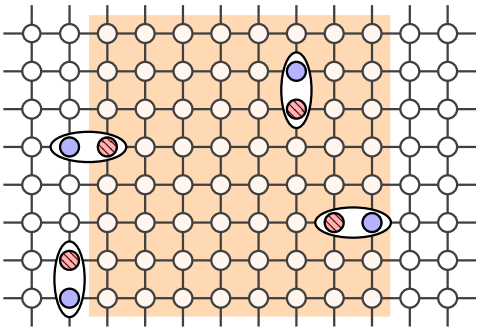

Figure 2. Cartoon of the 2D Mott insulator.

3. Insulating Phases of the 1D Hubbard Model Extended by Long-Range Interaction

3.1. The Extended Long-Range Hubbard Model

The one-dimensional extended Hubbard Model (EHM) is a lattice Hamiltonian describing the competition of kinetic energy and diagonal on-site (U) and nearest neighboring sites (V) density–density Coulomb interaction. Its applications range from high-T_c superconductors [25], to conducting polymers [26], organic charge-transfer salts [27], and ultracold atomic gases ([10] and references therein).

The full EHM phase diagram has been studied for specific fillings by means of different techniques [28–32]. In particular, the repulsive interaction regime ($U, V > 0$) has been intensively investigated due its physical relevance, and has a very rich structure, reported qualitatively in Figure 3 at half-filling. In this case, it amounts to three different insulating phases: a Mott insulator (Mott) characterized by dominant spin density waves, which takes place for U sufficiently greater than $2V$; a phase with BOW order [32], which appears for $U \approx 2V$; and a CDW phase, for U much smaller

than $2V$. While both BOW and CDW phases are fully gapped, and are thus associated to the ordering of appropriate local operators, the Mott insulating phase has no local order parameter. Remarkably, as shown in [5,14], NL operators are able to capture accurately and distinguish all three insulating regimes, as well as the transitions among them.

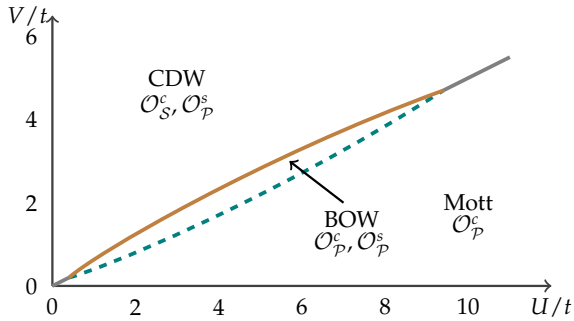

Figure 3. Phase diagram of the extended Hubbard model.

It is thus natural to ask how including terms further than nearest neighbors in the interaction, such as in the case of dipolar or Coulomb interaction, will affect the behavior of NL operators, as well as whether they will still behave as order parameters for the three distinct phases. To this end, we consider a generalized one-dimensional extended Hubbard model with L Fermions trapped in L lattice sites (half-filling), described by the following Hamiltonian

$$\begin{aligned} H &= -t\sum_{j,\sigma}\left(c^\dagger_{j\sigma}c_{j+1\sigma}+h.c.\right)+U\sum_j n_{j\uparrow}n_{j\downarrow} \\ &+ V\sum_{i,j}{}' \frac{\mathrm{e}^{-\lambda|i-j|}}{|i-j|^\alpha}n_i n_j \quad , \end{aligned} \tag{13}$$

where $\sigma = \uparrow, \downarrow$ is the spin index; $c^\dagger_{j\sigma}$ and $c_{j\sigma}$ are the Fermionic creation and annihilation operators, respectively; $n_{j\sigma} = c^\dagger_{j\sigma}c_{j\sigma}$ counts the number of particles with spin σ; and $n_j = \sum_\sigma n_{j\sigma}$. The coupling coefficients t, U describe the hopping process, and the on-site interaction, respectively, whereas V is the overall scale of the density–density interaction between further sites. Moreover, λ is its screening coefficient, and α is the exponent of its power law decay. Finally, the $'$ in the summation is reminiscent of the fact that in the numerical simulations it is limited to sites up to a given truncation distance R_T (in units of lattice constants): in other words, the summation is over pairs of sites (i, j) obeying the condition $1 \leq |i-j| \leq R_T \in \mathbf{N}$. For instance, the standard extended Hubbard model discussed at the beginning of this section amounts to the choice $R_T = 1$, $\lambda = 0$.

3.2. Results of DMRG Simulations

We applied the DMRG method [33,34] to observe the behavior of NL correlators in the Hamiltonian in Equation (13). In particular, we considered the case of the dipolar interaction ($\alpha = 3$, $\lambda = 0$) and that of the Coulomb interaction ($\alpha = 1$), both in the presence ($\lambda \neq 0$) and in the absence ($\lambda = 0$) of screening. The numerical simulations were performed on a chain of $L = 32$ sites with periodic boundary conditions, by keeping up to 1200 DMRG states and performing six sweeps to achieve convergence with a truncation error of 5×10^{-6}. Moreover, the long range interaction was truncated to the distance $R_T = 3$. The results, in the three cases, are shown in Figures 4–6, respectively, for fixed $(t, U) = (1, 4t)$ and changing V. In particular, the left side of each figure shows the charge correlators, while the right side refers to the spin channel. Here, we do not display the spin string,

which was always zero; instead, in addition to the spin parity $\mathcal{C}^s_{\mathcal{P}}$, we computed the Luttinger liquid parameter K_s defined as

$$K_s = \frac{4\pi}{L} \lim_{q \to 0} \frac{1}{q} \sum_{i,j} e^{\imath q(i-j)} \langle s_{si} s_{sj} \rangle \quad . \tag{14}$$

The charge string correlator $\mathcal{C}^c_{\mathcal{S}}(r)$ (first panel) was computed at the maximum distance, i.e., in the middle of the chain $r = L/2$. Instead, because of a possible staggered behavior, the parity correlators were averaged over the sites $L/2$ and $L/2 + 1$. In all cases, the results for the NL correlators support the presence of the three already mentioned phases, namely Mott, BOW and CDW, which can be inferred from the results in Figures 4–6, by taking into account the classification outlined in Table 1. The computation of K_s is helpful for identifying the transitions. In particular, the Mott–BOW transition, which involves the opening of the spin gap, is signaled by $K_s = 1$. We observed that, in all the figures, the BOW phase appears slightly shifted from the point $U \approx 2V$ towards higher values of V; thus, the long-range interaction basically does not alter the phase diagram of the EHM. We noticed that, in the case of screened Coulomb repulsion, the amplitude of the interaction must be scaled by the factor $e^{-\lambda}$ in order to compare the result with the EHM. We chose $\lambda = 0.7$ in such a way that the contribution from the fourth nearest neighbors, which we neglect, is of the same order as the contribution neglected for dipolar interaction. Such a choice should make the screened Coulomb interaction comparable to the case $\alpha > 1$, for which it is known that the long-range interaction does not qualitatively modify the phase diagram [9]. We verified that the results are barely affected by the truncation of the long range interaction. To this end, we considered the screened Coulomb interaction truncated to $R_T = 5$. In that case, we assumed, with the same criterion, $\lambda = 0.6$. Data are shown in Figure 7. We performed the computation for a system of size $L = 24$, with up to 1400 DMRG states and eight sweeps. We observed that the results are comparable with those obtained for the case $R_T = 3$. In fact, the BOW phase appears closer to the point $U = 2V$; however, this small difference could also be caused either by finite size effects or by the difficulty of DMRG in reaching convergence despite the eight sweeps. On the other hand, in the case of dipolar interaction, one may infer, by comparison with the work in [35], where up to five neighbors are included, that the transition lines are not much affected by adding further neighbors to the interaction or by increasing the system size from $L = 32$ to the thermodynamic limit. These findings complement those reported in the previous literature [36,37]. On the contrary, we expect that, in the case of unscreened long-range Coulomb interaction ($\alpha = 1$), an increase of R_T could modify our results, since the neglected terms in the present analysis are much higher than in the other cases, and the analytic results on the persistence of the phases are controversial [38,39].

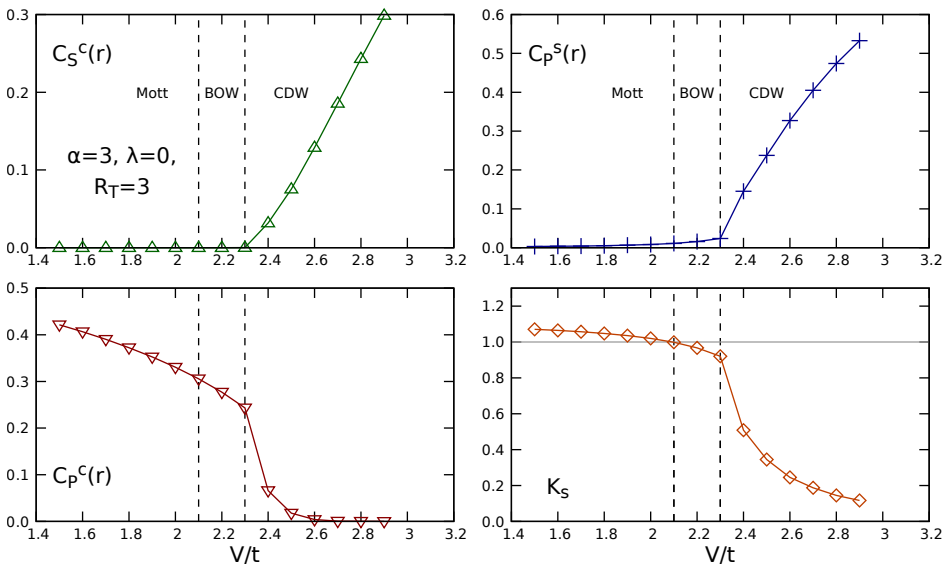

Figure 4. Behavior of the non-local correlation functions in Equation (5) and the Luttinger liquid parameter K_s for the Hamiltonian in Equation (13) with dipolar interaction ($\alpha = 3$, $\lambda = 0$) truncated to third nearest neighbors ($R_T = 3$) at $t = 1$ and $U = 4t$. The simulations were performed with finite DMRG for a chain of length $L = 32$, by keeping up to 1200 states and performing six sweeps. The string operator was computed in the middle of the chain $r = L/2$, while the parity operators were averaged between the two central points $L/2$ and $L/2 + 1$.

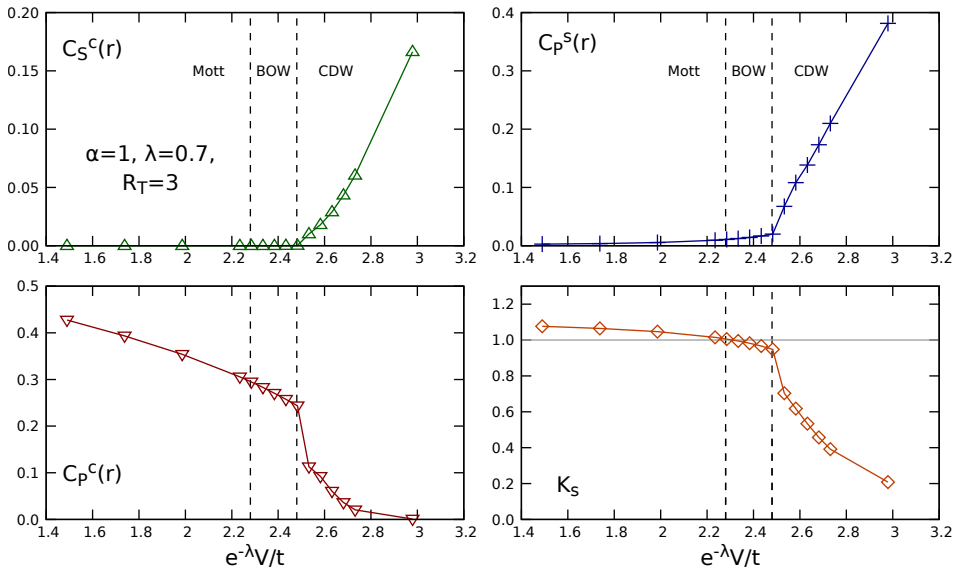

Figure 5. Behavior of the non-local correlation functions in Equation (5) and the Luttinger liquid parameter K_s for the Hamiltonian in Equation (13) with screened Coulomb interaction ($\alpha = 1$, $\lambda = 0.7$) truncated to third nearest neighbors ($R_T = 3$) at $t = 1$ and $U = 4t$. The simulations were performed with finite DMRG for a chain of length $L = 32$, by keeping up to 1200 states and performing six sweeps. The string operator was computed in the middle of the chain $r = L/2$, while the parity operators were averaged between the two central points $L/2$ and $L/2 + 1$.

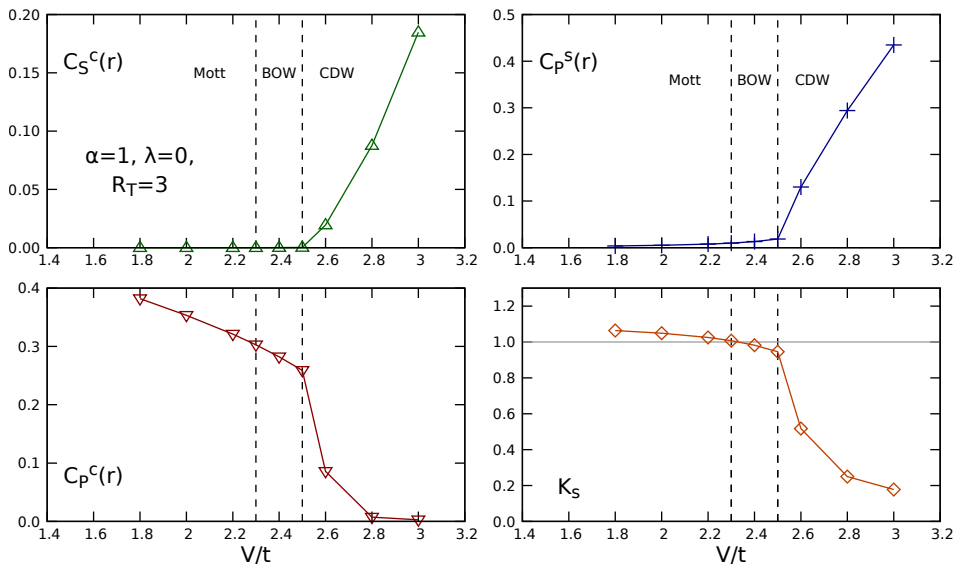

Figure 6. Behavior of the non-local correlation functions in Equation (5) and the Luttinger liquid parameter K_s for the Hamiltonian in Equation (13) with Coulomb interaction ($\alpha = 1$, $\lambda = 0$) truncated to third nearest neighbors ($R_T = 3$) at $t = 1$ and $U = 4t$. The simulations were performed with finite DMRG for a chain of length $L = 32$, by keeping up to 1200 states and performing six sweeps. The string operator was computed in the middle of the chain $r = L/2$, while the parity operators were averaged between the two central points $L/2$ and $L/2 + 1$.

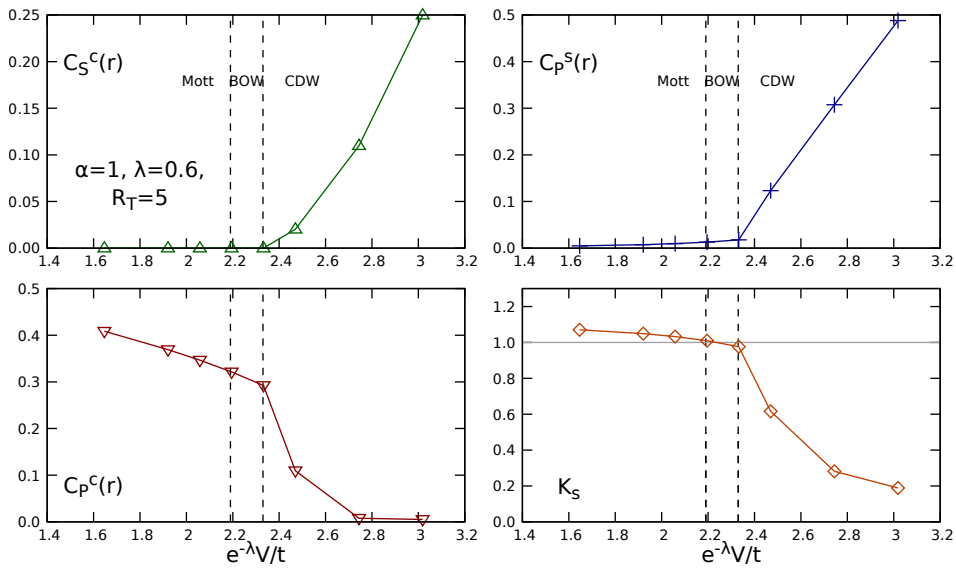

Figure 7. Behavior of the non-local correlation functions in Equation (5) and the Luttinger liquid parameter K_s for the Hamiltonian in Equation (13) with screened Coulomb interaction ($\alpha = 1$, $\lambda = 0.6$) truncated to fifth nearest neighbors ($R_T = 5$) at $t = 1$ and $U = 4t$. The simulations were performed with finite DMRG for a chain of length $L = 24$, by keeping up to 1400 states and performing eight sweeps. The string operator was computed in the middle of the chain $r = L/2$, while the parity operators were averaged between the two central points $L/2$ and $L/2 + 1$.

4. Conclusions

In this paper, we review some results on the capability of hidden non-local orders, described by string and parity operators, of giving an exhaustive characterization of the insulating states induced by short range interaction in low-dimensional Fermionic materials. We have seen how, in the absence of disorder, in one dimension the classification of the insulating phases by non-local

orders is possible thanks to the characteristic spin–charge separation of the degrees of freedom involved. Moreover, we discuss how the insulating state associated to the parity operator, which is trivial from the topological point of view, persists in two dimensions and is still characterized by a generalized parity operator: the physics remains the same. In addition, we show that instead the insulating states associated to the ordering of the string operators are characterized in one dimension by non-trivial topological properties, notably the non-unity, degenerate, fractional and entangled edge charges.

Finally, we applied the previous framework to a preliminary study of the effect of various long ranged interaction added to the extended Hubbard model. The study was performed at finite size and a representative value of the on-site interaction $U = 4t$, half-filling and zero magnetization. By means of DMRG numerical simulations, we investigated the changes in the behavior of the non-local parameters and phase transition lines, by varying the density-density interaction scale in the case of dipolar, screened and unscreened interactions, respectively. Our results suggest that all three phases of the EHM (Mott, BOW, and CDW) are robust in the presence of an interaction range beyond one lattice cell, both transitions still occurring in proximity of the value $U = 2V$. Moreover, the non-local parity and string charge operators are still capable of describing the transitions.

We observed that, in the case of dipolar interaction, a further increase of the truncation distance R_T is not believed to affect sensibly the phase diagram. The same can be expected in the case of screened Coulomb interaction for suitable choices of λ. On the contrary, different results may be observed if an unscreened long-range Coulomb repulsion is considered, upon including a sufficiently large number of neighbors. Further investigations go beyond the aim of this review.

Author Contributions: Both authors have contributed equally to the research.

Funding: This research received no external funding.

Conflicts of Interest: The authors declare no conflicts of interest.

References

1. Mott, N.F. *Metal Insulator Transition*; Taylor & Francis: London, UK, 1990.
2. Montorsi, A.; Roncaglia, M. Nonlocal Order Parameters for the 1D Hubbard Model. *Phys. Rev. Lett.* **2012**, *109*, 236404. [CrossRef] [PubMed]
3. Boschi, C.D.E.; Montorsi, A.; Roncaglia, M. Brane parity orders in the insulating state of Hubbard ladders. *Phys. Rev. B* **2016**, *94*, 085119. [CrossRef]
4. Fazzini, S.; Becca, F.; Montorsi, A. Nonlocal parity order in the two-dimensional Mott insulator. *Phys. Rev. Lett.* **2017**, *118*, 157602. [CrossRef] [PubMed]
5. Barbiero, L.; Montorsi, A.; Roncaglia, M. How hidden orders generate gaps in one-dimensional fermionic systems. *Phys. Rev. B* **2013**, *88*, 035109. [CrossRef]
6. Dolcini, F.; Montorsi, A. Quantum phases of one-dimensional Hubbard models with three-and four-body couplings. *Phys. Rev. B* **2013**, *88*, 115115. [CrossRef]
7. Endres, M.; Cheneau, M.; Fukuhara, T.; Weitenberg, C.; Schauß, P.; Gross, C.; Mazza, L.; Bañuls, M.C.; Pollet, L.; Bloch, I.; et al. Observation of Correlated Particle-Hole Pairs and String Order in Low-Dimensional Mott Insulators. *Science* **2011**, *334*, 200. [CrossRef] [PubMed]
8. Hilker, T.A.; Salomon, G.; Grusdt, F.; Omran, A.; Boll, M.; Demler, E.; Bloch, I.; Gross, C. Revealing hidden antiferromagnetic correlations in doped Hubbard chains via string correlators. *Science* **2017** *357*, 484. [CrossRef]
9. Giamarchi, T. *Quantum Physics in One Dimension*; Oxford University Press: Oxford, UK, 2003.
10. Fazzini, S.; Montorsi, A.; Barbiero, L. Low energy quantum regimes of 1D dipolar Hubbard model with correlated hopping. *J. Phys. Conf. Ser.* **2017**, *841*, 012016. [CrossRef]
11. Gogolin, A.O.; Nersesyan, A.A.; Tsvelik, A.M. *Bosonization and Strongly Correlated Systems*; Cambridge University Press: Cambridge, UK, 1998.
12. Japaridze, G.I.; Kampf, A.P. Weak-coupling phase diagram of the extended Hubbard model with correlated-hopping interaction. *Phys. Rev. B* **1999**, *59*, 12822. [CrossRef]
13. Nakamura, M. Tricritical behavior in the extended Hubbard chains. *Phys. Rev. B* **2000**, *61*, 16377. [CrossRef]

14. Barbiero, L.; Fazzini, S.; Montorsi, A. Non-local order parameters as a probe for phase transitions in the extended Fermi-Hubbard model. *Eur. Phys. J. Spec. Top.* **2017**, *226*, 2697. [CrossRef]
15. Barbiero, L.; Fazzini, S.; Montorsi, A.; Roncaglia, M. Hidden magnetism in periodically modulated one dimensional dipolar fermions. *New J. Phys.* **2017**, *19*, 123008.
16. Aligia, A.A.; Arrachea, L. Triplet superconductivity in quasi-one-dimensional systems. *Phys. Rev. B* **1999**, *60*, 15332. [CrossRef]
17. Berg, E.; Torre, E.G.D.; Giamarchi, T.; Altman, E. Rise and fall of hidden string order of lattice bosons. *Phys. Rev. B* **2008**, *77*, 245119. [CrossRef]
18. Montorsi, A.; Dolcini, F.; Iotti, R.; Rossi, F. Symmetry-protected topological phases of one-dimensional interacting fermions with spin-charge separation. *Phys. Rev. B* **2017**, *95*, 245108. [CrossRef]
19. Gu, Z.-C.; Wen, X.-G. Tensor-entanglement-filtering renormalization approach and symmetry-protected topological order. *Phys. Rev. B* **2009**, *80*, 155131. [CrossRef]
20. Chen, X.; Gu, Z.-C.; Liu, Z.-X.; Wen, X.-G. Symmetry-Protected Topological Orders in Interacting Bosonic Systems. *Science* **2012**, *338*, 1604. [CrossRef] [PubMed]
21. Pollmann, F.; Turner, A.M.; Berg, E.; Oshikawa, M. Entanglement spectrum of a topological phase in one dimension. *Phys. Rev. B* **2010**, *81*, 064439. [CrossRef]
22. Pollmann, F.; Berg, E.; Turner, A.M.; Oshikawa, M. Symmetry protection of topological phases in one-dimensional quantum spin systems. *Phys. Rev. B* **2012**, *85*, 075125. [CrossRef]
23. Rath, S.P.; Simeth, W.; Endres, M.; Zwerger, W. Non-local order in Mott insulators, duality and Wilson loops. *Ann. Phys. (N. Y.)* **2013**, *334*, 256. [CrossRef]
24. Tocchio, L.; Becca, F.; Montorsi, A. Superconductivity in the Hubbard model: A hidden-order diagnostics from the Luther-Emery phase on ladders. *SciPost Phys.* **2019**, *6*, 018. [CrossRef]
25. Emery, V.J.; Kivelson, S.A.; Zachar, O. Spin-gap proximity effect mechanism of high-temperature superconductivity. *Phys. Rev. B* **1997**, *56*, 6120. [CrossRef]
26. Keiss, H.G. *Conjugated Conducting Polymers*; Springer: Berlin, Germany, 1992.
27. Ishiguro, T.; Yamaji, K. *Organic Superconductors*; Springer: Berlin, Germany, 1990.
28. Hirsch, J.E. Charge-density-wave to spin-density-wave transition in the extended Hubbard model. *Phys. Rev. Lett.* **1984**, *53*, 2327. [CrossRef]
29. Lin, H.Q.; Hirsch, J.E. Condensation transition in the one-dimensional extended Hubbard model. *Phys. Rev. B* **1986**, *33*, 8155. [CrossRef]
30. Cannon, J.W.; Fradkin, E. Phase diagram of the extended Hubbard model in one spatial dimension. *Phys. Rev. B* **1990**, *41*, 9435. [CrossRef]
31. Penc, K.; Mila, F. Phase diagram of the one-dimensional extended Hubbard model with attractive and/or repulsive interactions at quarter filling. *Phys. Rev. B* **1994**, *49*, 9670. [CrossRef]
32. Nakamura, M. Mechanism of CDW-SDW transition in one dimension. *J. Phys. Soc. Jpn.* **1999**, *68*, 3123. [CrossRef]
33. White, S.R. Density matrix formulation for quantum renormalization groups. *Phys. Rev. Lett.* **1992**, *69*, 2863. [CrossRef] [PubMed]
34. Schollwöck, U. The density-matrix renormalization group. *Rev. Mod. Phys.* **2005** *77*, 259. [CrossRef]
35. Dio, M.D.; Barbiero, L.; Recati, A.; Dalmonte, M. Spontaneous Peierls dimerization and emergent bond order in one-dimensional dipolar gases. *Phys. Rev. A* **2014**, *90*, 063608. [CrossRef]
36. Hauke, P.; Cucchietti, F.M.; Müller-Hermes, M.; Bañuls, A.; Cirac, J.I.; Lewenstein, M. Complete devil's staircase and crystal–superfluid transitions in a dipolar XXZ spin chain: a trapped ion quantum simulation. *New J. Phys.* **2010**, *12*, 113037. [CrossRef]
37. Peter, D.; Müller, S.; Wessel, S.; Büchler, H.P. Anomalous behavior of spin systems with dipolar interactions. *Phys. Rev. Lett.* **2012**, *109*, 025303. [CrossRef] [PubMed]
38. Vodola, D.; Lepori, L.; Ercolessi, E.; Pupillo, G. Long-range Ising and Kitaev models: phases, correlations and edge modes. *New J. Phys.* **2016** *18*, 0150001. [CrossRef]
39. Frérot, I.; Naldesi, P.; Roscilde, T. Entanglement and fluctuations in the XXZ model with power-law interactions. *Phys. Rev. B* **2017** *95*, 245111. [CrossRef]